Supplementary Information for:

Evaluating the Photophysical and Photochemical Characteristics of

Green-Emitting Cerium(III) Mono-Cyclooctatetraenide Complexes

Pragati Pandey,[a] Qiaomu Yang,[a] Michael R. Gau,[a] and Eric J. Schelter[a]*

[a]P. Roy and Diana T. Vagelos Laboratories, Department of Chemistry, University of Pennsylvania, 231 South 34 Street, Philadelphia, Pennsylvania 19104, United States

schelter@sas.upenn.edu

Table of Contents

Figure S1: ^{1}H NMR (THF-d_8) spectrum of **1**.

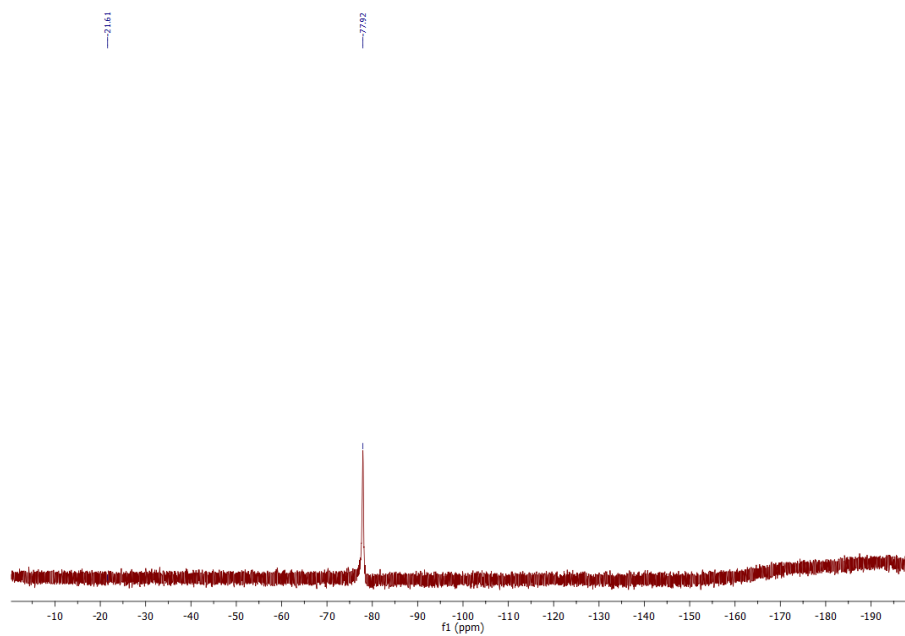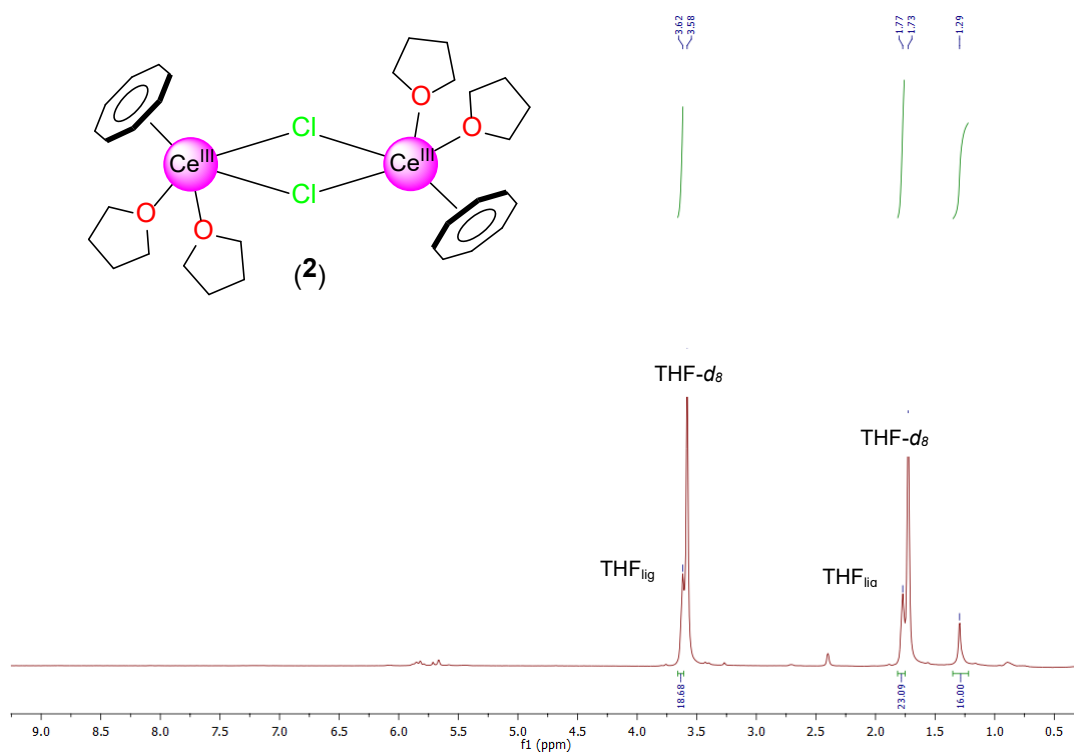**Figure S2:** ^{19}F NMR (THF-d_8) spectrum of **1**.

Figure S3: ^{1}H NMR (THF-d_8) spectrum of **2**.
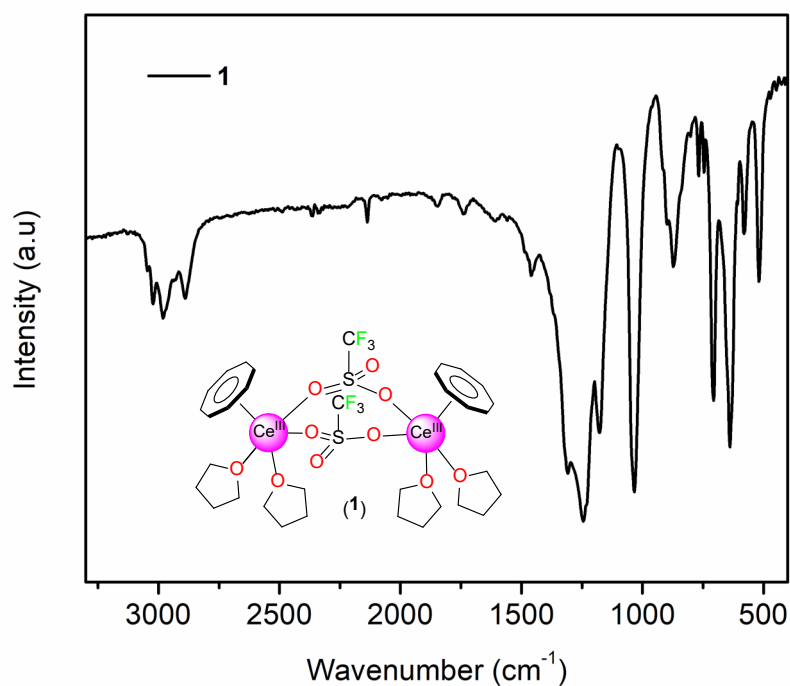
Figure S4. FT-IR spectra of **1** in KBr pellet.
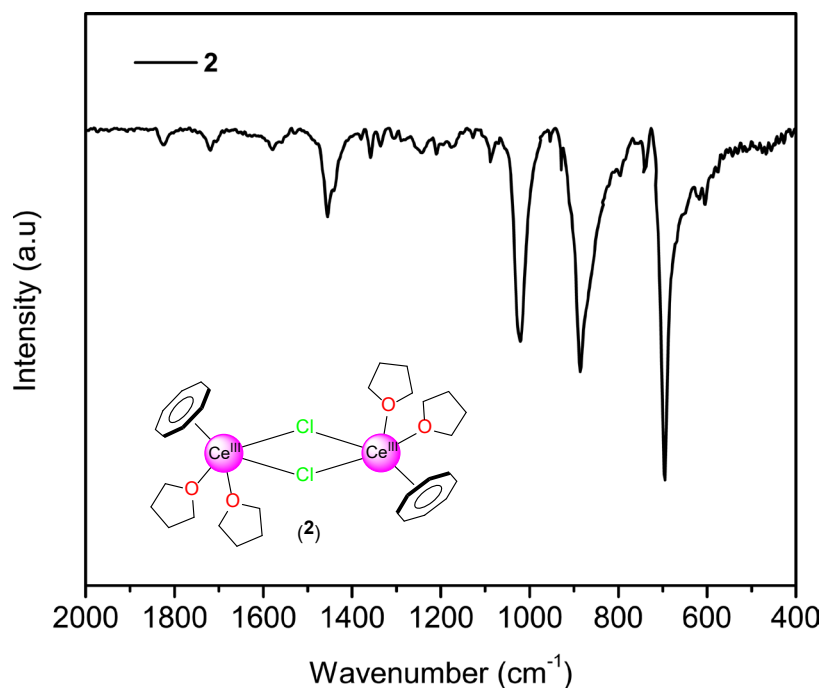
Figure S5. FT-IR spectra of **2** in KBr pellet. (The characteristic stretching frequency (1010 cm^{-1}) for coordinated THF molecules is observed towards higher wavenumber (1015 cm^{-1}) due to the presence of free THF solvent molecules).

Complex	1		2	
	Reported Data[1]	New Data	Reported Data[2]	New Data
	2136 m	3045 m	1070 (w)	1091 (w)
	1740 m	3022 m	1010 (s)	1015 (s)
	1308 m	2982 m	965 (w)	927 (w, sh)
	1245 sst	2889 m	918 (w, sh)	796 (w)
	1230 sst	2137 m	885 (s)	739 (w)
	1097 m	1740 w	792 (w)	887 (s)
	1032 sst	1460 w	736 (w)	693 (vs)
	978 m	1309 m	715 (w, sh)	
	918 m	1244 s	703 (sh)	
	871 st	1230 s	694 (vs)	
	761 m	1097 w		
	712 st	1034 s		
	638 st	913 w		
	579 m	873 s		
	519 st	767 m		
		706 s		
		638 s		
		579 m		
		518 s		

Table S2 IR data for the complexes **1** and **2**

2. X-ray Crystallography. X-ray intensity data were collected on a Rigaku XtaLAB Synergy-S diffractometer[3] equipped with an HPC area detector (Dectris Pilatus3 R 200 K) and employing confocal multilayer optic-monochromated Mo-Kα radiation (λ=0.71073 Å) at a temperature of 160K. Preliminary indexing was performed from a series of thirty 0.5° rotation frames with exposures of 0.25 seconds. A total of 1202 frames (13 runs) were collected employing ω scans with a crystal to detector distance of 34.0 mm, rotation widths of 0.5° and exposures of 4 seconds.

Rotation frames were integrated using CrysAlisPro[4] producing a listing of unaveraged F^2 and $\sigma(F^2)$ values. A total of 82455 reflections were measured over the ranges $4.512 \leq 2\theta \leq 56.564°$, $-26 \leq h \leq 26$, $-17 \leq k \leq 16$, $-24 \leq l \leq 24$ yielding 10185 unique reflections (Rint = 0.0496). The intensity data were corrected for Lorentz and polarization effects and for absorption using SCALE3 ABSPACK[5] (minimum and maximum transmission 0.62230, 1.00000). The structure was solved by dual space methods - SHELXT (Sheldrick, 2018)[6]. Refinement was by full-matrix least squares based on F^2 using SHELXL[7]. All reflections were used during refinement. The weighting scheme used was $w=1/[\sigma^2(F_o^2)+ (0.0272P)^2 + 6.1081P]$ where $P = (F_o^2 + 2F_c^2)/3$. Non-hydrogen atoms were refined anisotropically and hydrogen atoms were refined using a riding model.

Table S2 Crystallographic data and refinement parameters for complex **1**

Empirical formula	$C_{34}H_{48}Ce_2F_6O_{10}S_2$
Formula weight	1075.08
Diffractometer	Rigaku XtaLAB Synergy-S (Dectris Pilatus3 R 200K)
Temperature/K	160
Crystal system	monoclinic
Space group	$P2_1/c$
a	19.8941(7)Å
b	12.7812(4)Å
c	18.0563(6)Å
α	90°
β	116.481(4)°
γ	90°
Volume	4109.5(3)Å^3
Z	4
d_{calc}	1.738 g/cm^3
μ	2.367 mm^{-1}
F(000)	2136.0
Crystal size, mm	0.36 × 0.11 × 0.06
2θ range for data collection	4.512 - 56.564°
Index ranges	-26 ≤ h ≤ 26, -17 ≤ k ≤ 16, -24 ≤ l ≤ 24
Reflections collected	82455
Independent reflections	10185[R(int) = 0.0496]
Data/restraints/parameters	10185/213/532
Goodness-of-fit on F^2	1.037
Final R indexes [I>=2σ (I)]	$R_1 = 0.0320$, $wR_2 = 0.0698$
Final R indexes [all data]	$R_1 = 0.0410$, $wR_2 = 0.0726$
Largest diff. peak/hole	1.10/-0.55 eÅ^{-3}

Table S3 New Crystallographic data for complex $[(C_8H_8)Ce(\mu\text{-Cl})(THF)_2]_2$ (**2**)
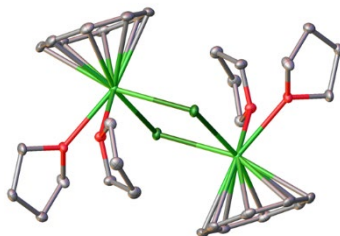
Reported unit cell parameters for **2** from CCDC data base[8]	New unit cell parameters for **2**	
Monoclinic, P21/c	Triclinic, P1	Monoclinic, P21/n
a = 11.86 (Å)	a = 8.77 (Å),	a = 11.71 (Å)
b = 12.62 (Å)	b = 8.89(Å),	b = 12.76 (Å)
c = 13.49 (Å)	c = 11.74 (Å)	c = 11.88 (Å)
α = 90°	α = 92.89°	α = 90°
β = 122.91°	β = 108.47°	β = 113.58°
γ = 90°	γ = 102.37°	γ = 90°
V = 1697.38 (Å^3)	V = 841.96 (Å^3)	V = 1629.12 (Å^3)

3. Photophysical Studies

Absorption and Emission Spectroscopy. 10 mm path length quartz cells fused with a J-Young valve were used for UV-vis and luminescence studies of air and moisture sensitive compounds.[9] Electronic absorption spectra (UV-Vis) were collected on a Perkin Elmer 950 UV-Vis/NIR spectrophotometer. Emission and excitation spectra were collected on Fluorolog®-3 spectrofluorometer (HORIBA Jobin Yvon, Inc.) using an R928 PMT detector. Solid state photoluminescence of **1** and **2** were collected in screw cap 1 mm cuvette. Lifetime measurements were performed on a PTI PicoMaster TCSPC lifetime fluorometer with a 455 nm wavelength source.

Absolute photoluminescence quantum yields (PLQY) measurement: Absolute PLQYs were measured using JASCO spectrofluorometer FP-8300 with ILF-835 100 mm diameter Integrating Sphere system. All measurements were performed at room temperature by using 1 mm screw cap cuvette. To calibrate the instrument absolute PLQY for fluoresceine in 0.1 N NaOH solution was measured with $\Phi_{flu} = 0.89$.[10,11,12] For each Quantum Yield measurement, the incident excitation light spectrum was collected in the presence of 0.5 mL of THF solvent. After measuring the incident light intensity, the new fluorescence spectrum (fluorescence intensity and new incident light intensity) of **1** (1.0 mM) and **2** (~1.0 mM) in THF were collected with excitation at 450 nm. Using the JASCO Yield Software FWQE-880 Quantum Yield Calculation program, quantum yield was calculated by dividing the complex fluorescence intensity by the difference in incident light intensity in the presence and absence of complex.
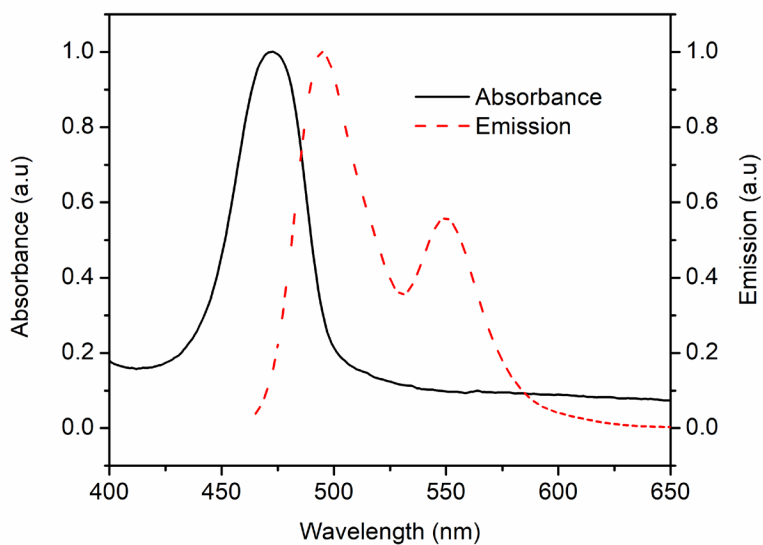
Figure S6: Normalized absorbance (black solid) and emission (red dash) spectra of complex **1** with Stokes shift 0.122 eV (23 nm) in THF solution.
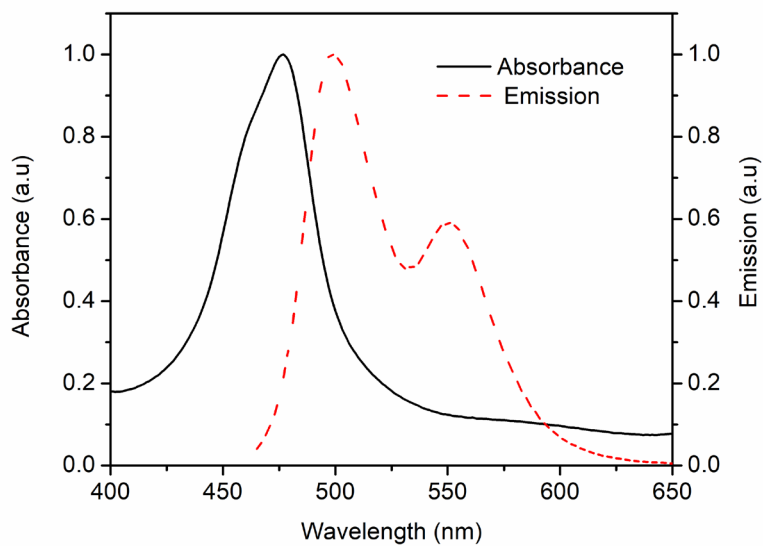

Figure S7: Normalized absorbance (black solid) and emission (red dash) spectra of complex **1** with Stokes shift 0.115 eV (22 nm) in THF solution.
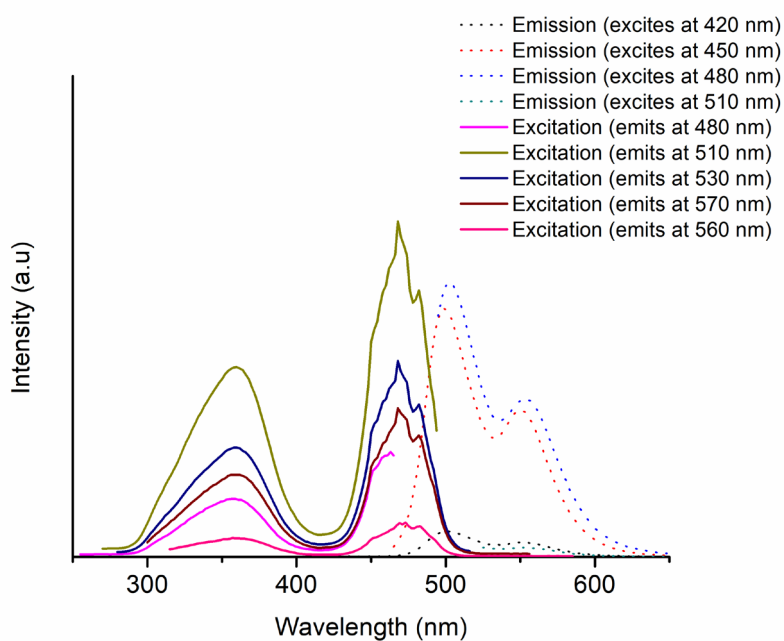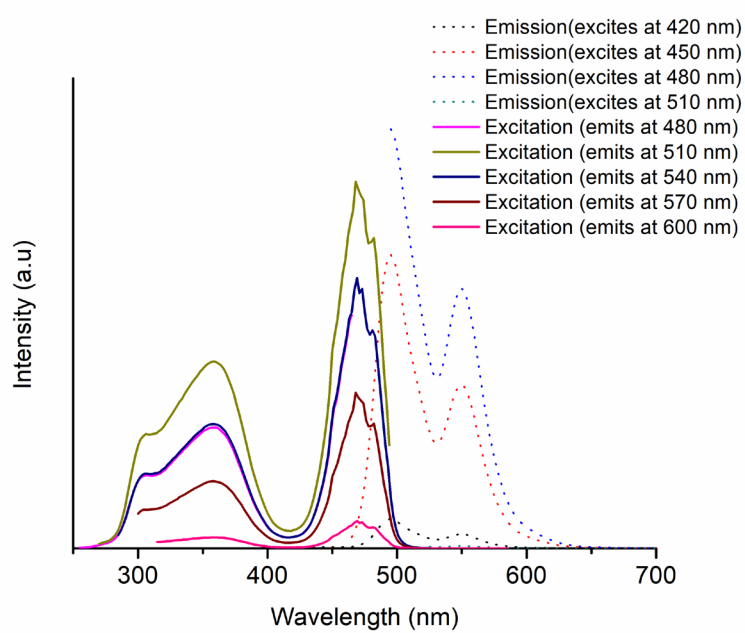
Figure S8. Photoluminescence spectra of **1** (top) and **2** (bottom) in THF solution at different excitation and emission wavelengths.
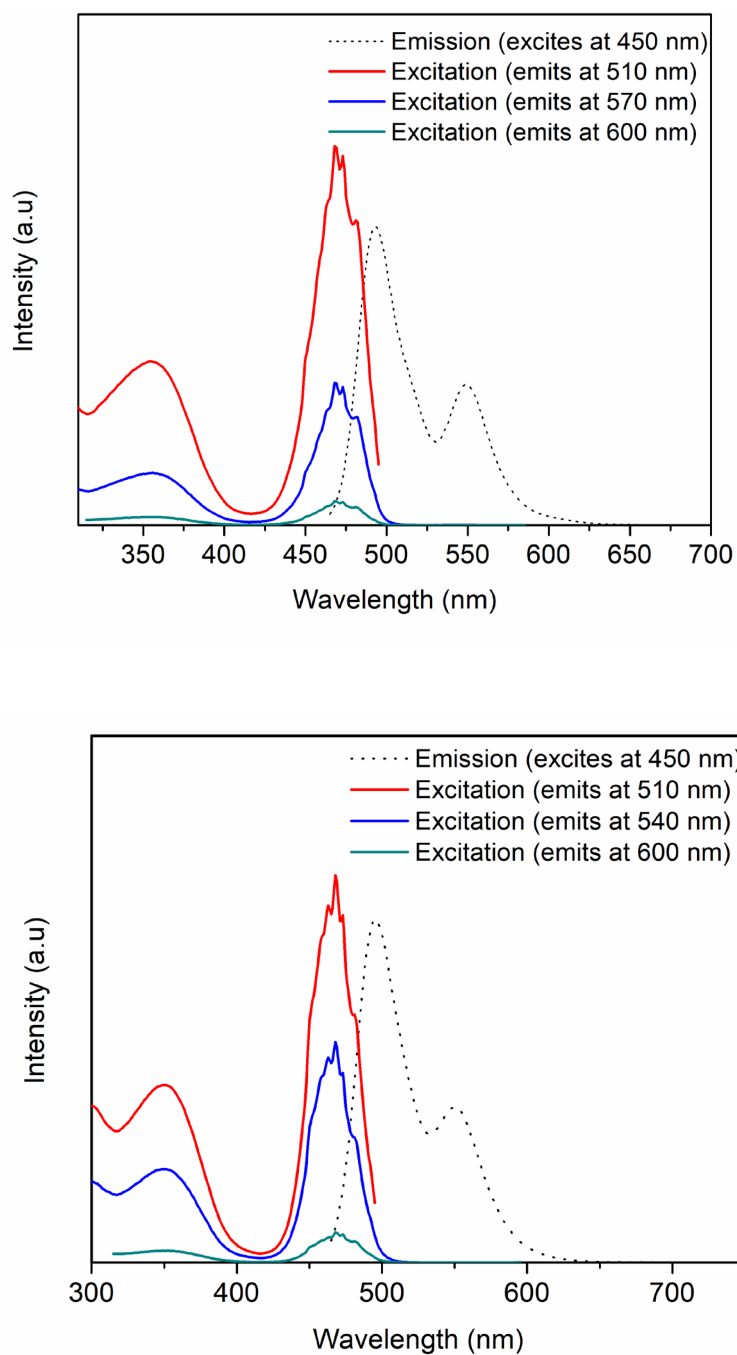
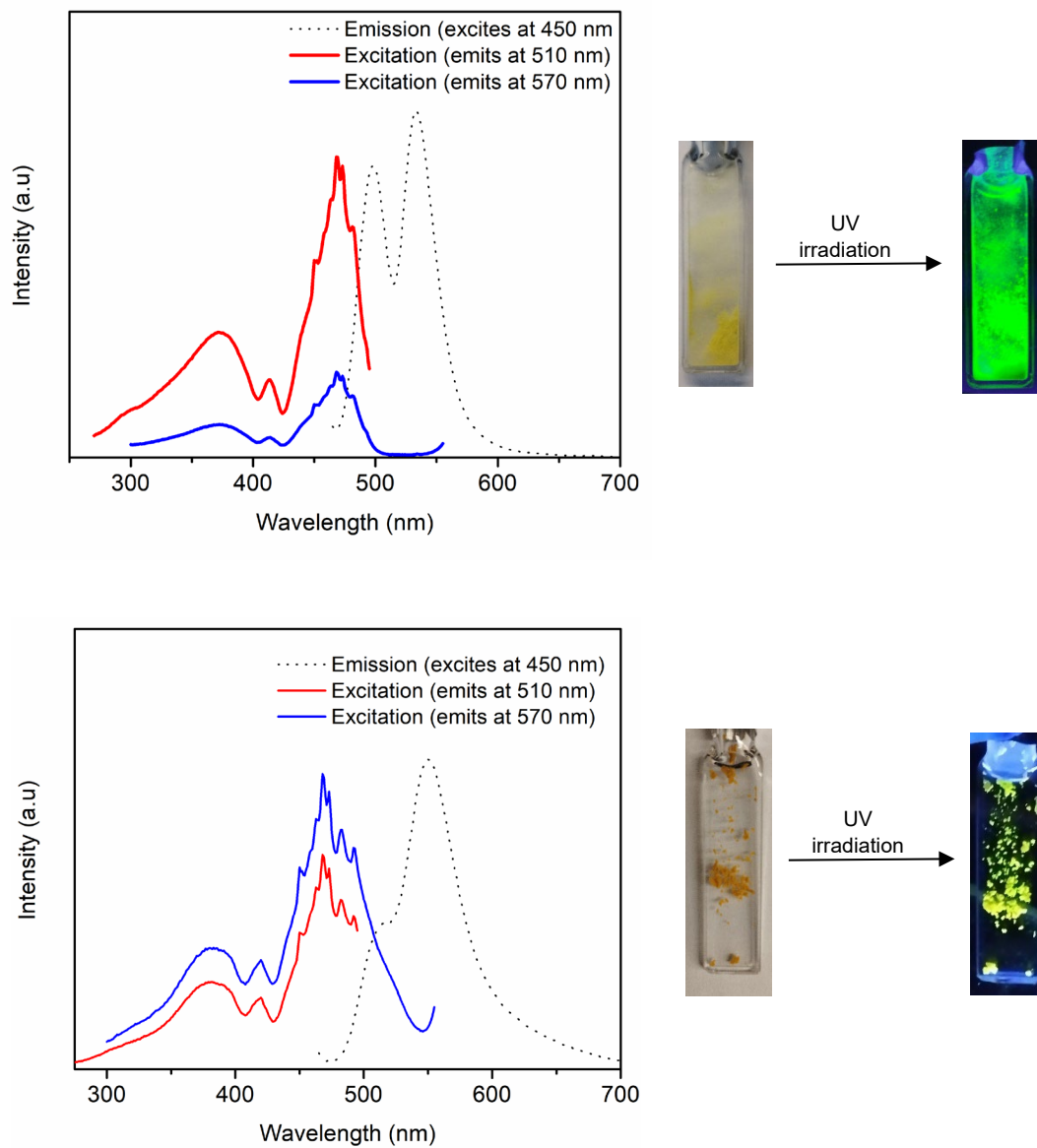**Figure S9**. Photoluminescence spectra of **1** (top) and **2** (bottom) in THF solution (0.25 mM) with absorbance ca <0.2.

Figure S10. Solid state photoluminescence spectra of **1** (top) and **2** (bottom).
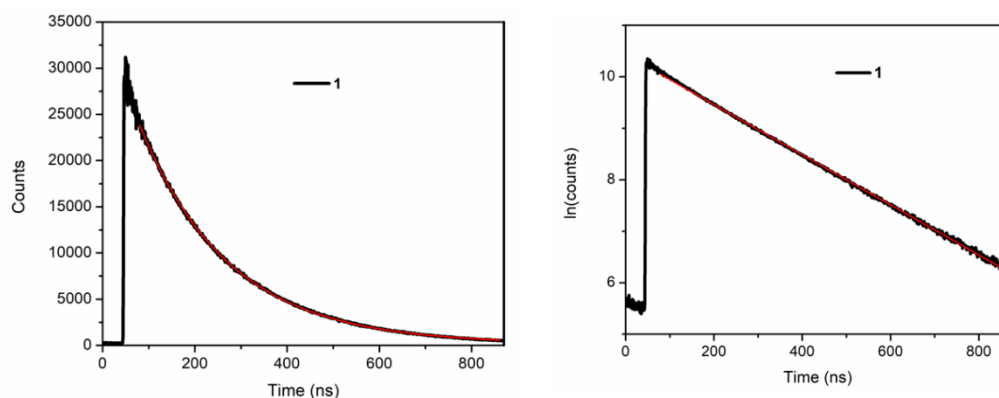
Figure S11. (Left) Time-resolved emission intensity decay of **1** in THF shown in black trace. The decay data was collected at 480 nm with 455 nm excitation. A single exponential fit from 80 ns to 860 ns is given a red line, affording τ = 205.4± 0.2 ns. (Right) The ln(counts) versus time plot of time-resolved emission intensity decay for **1** in THF is shown in the black trace with the model shown as the red solid line (R^2 = 0.999).
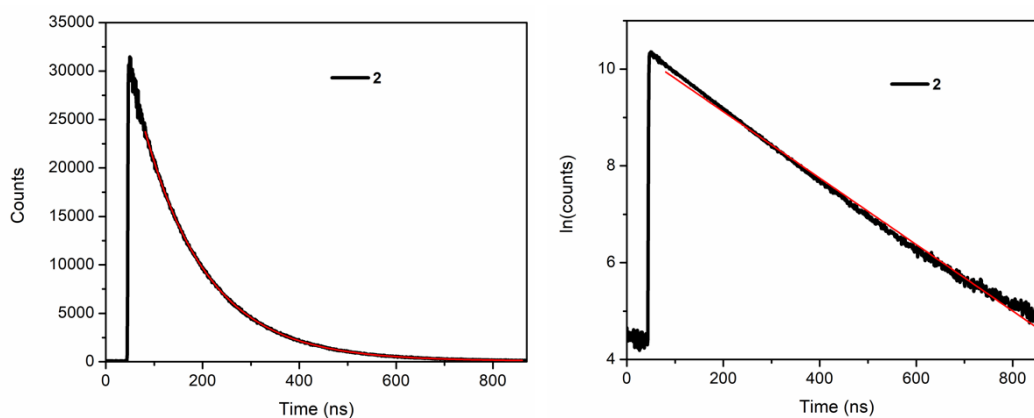

Figure S12. (Left) Time-resolved emission intensity decay of **2** in THF shown in black trace. The decay data was collected at 480 nm with 455 nm excitation. A single exponential fit from 80 ns to 860 ns is given as a red line, affording τ = 145.8 ± 0.4 ns. (Right) the ln(counts) versus time plot of time-resolved emission intensity decay for **2** in THF is shown in the black trace with the model shown as the red solid line (R^2 = 0.995).
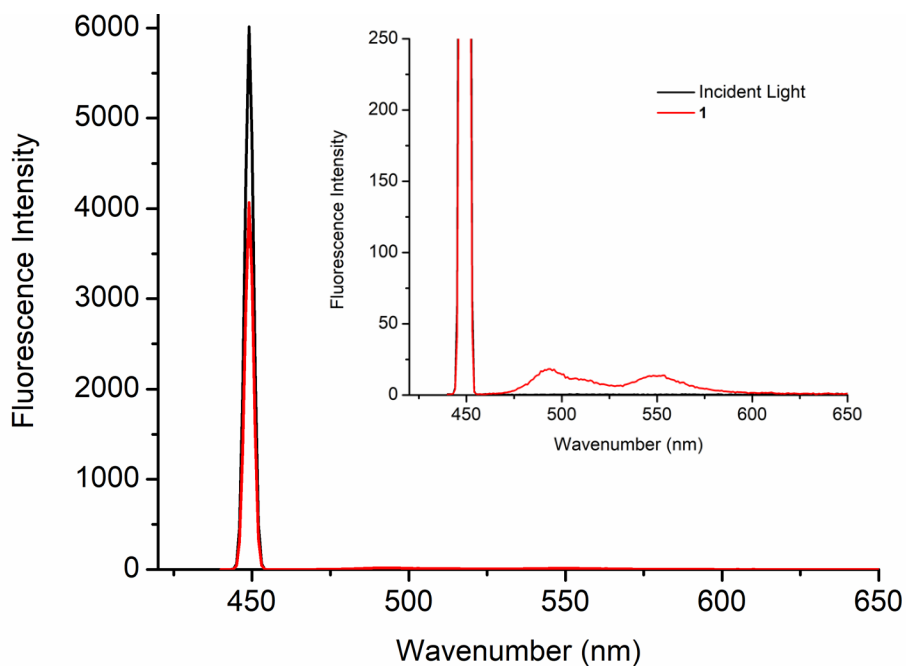
Figure. S13. PLQY spectrum for **1** in THF (1.0 mM) with excitation at 450 nm and a spectral collection range of 440-650. Inset figure shows the emission bands for **1**.
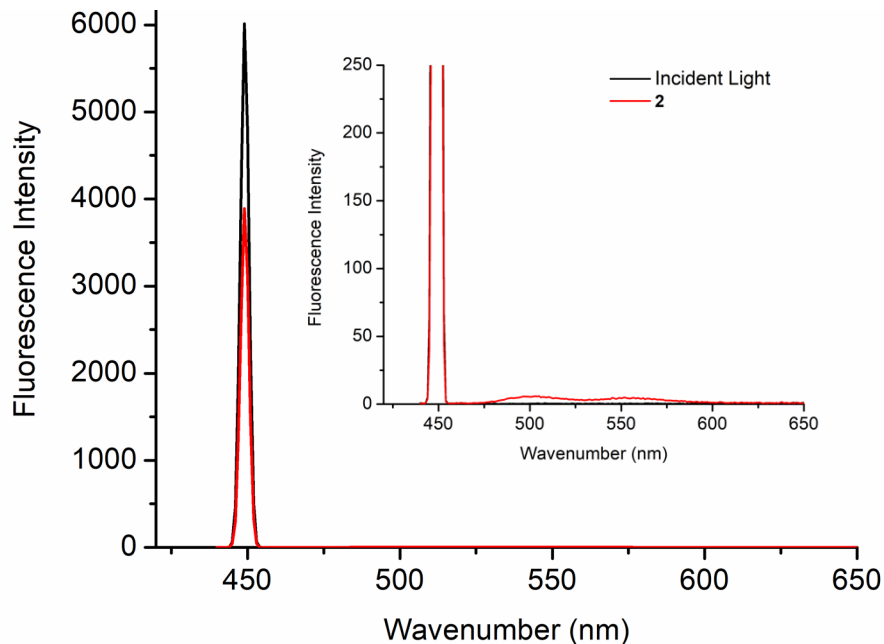

Figure. S14. PLQY spectrum for **2** in THF (1.0 mM) with excitation at 450 nm and spectral collection range of 440-650. Inset figure shows the emission bands for **2.**
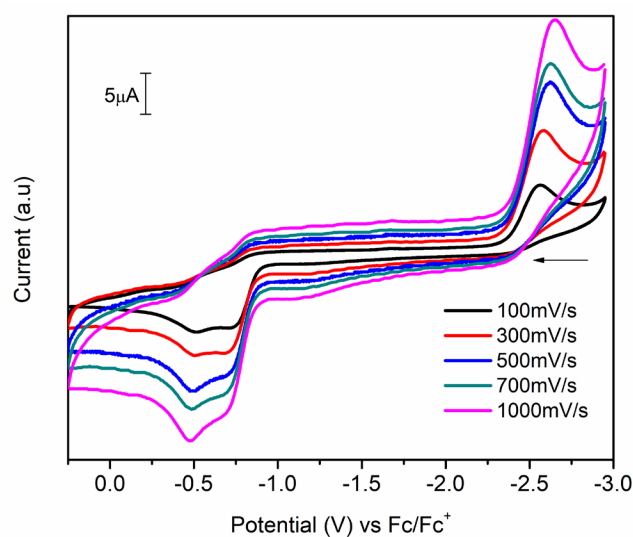
4. Electrochemistry

Figure S15. Scan rate dependent study of **1**. Solvent: THF; electrolyte 0.1 M [^{n}Pr$_4$N][BAr$^F_4$]; [analyte] = 0.002 M. anodic scan was started from −3.0 V.

Figure S16: Differential pulse voltammetry of **1** (0.002 M) recorded in THF using [^{n}Pr$_4$N][BAr$^F_4$] (0.1 M) as the supporting electrolyte.
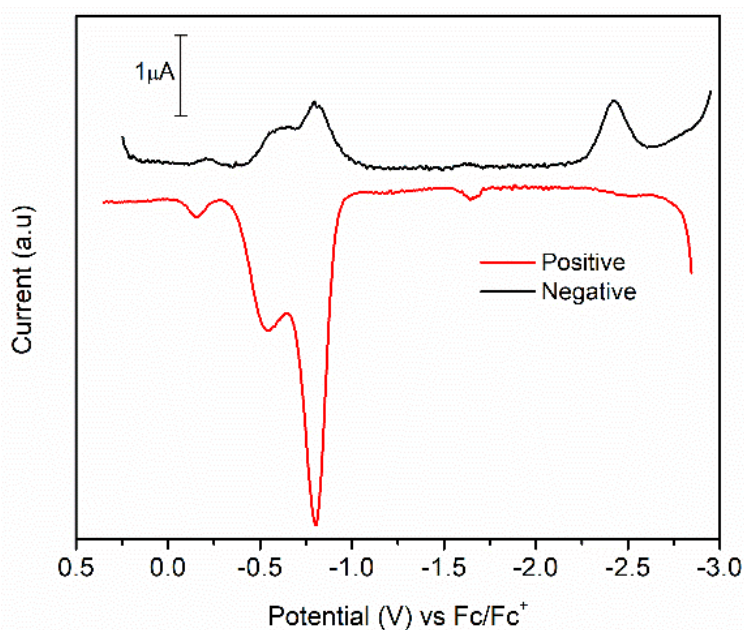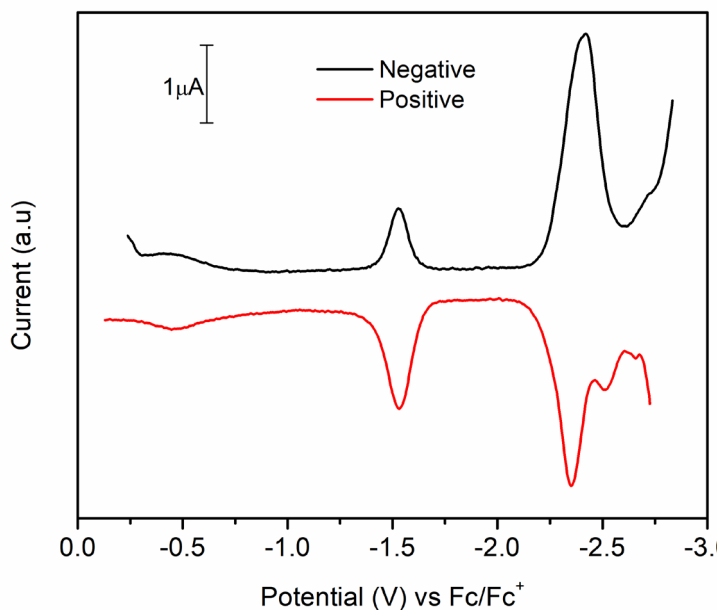
Figure S17: Differential pulse voltammetry of **1** (0.002 M) recorded in THF using [^{n}Pr$_4$N][BAr$^F_4$] (0.1 M) as the supporting electrolyte.
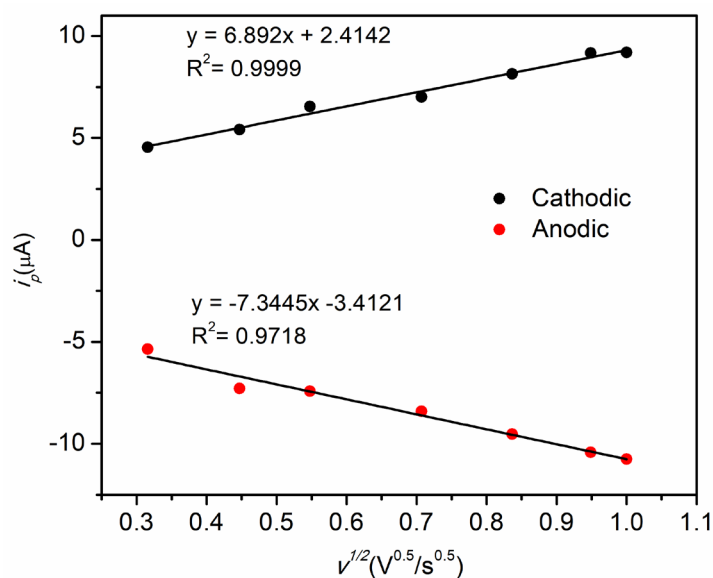

Figure S18: Plot of the square of the scan rate ($v^{1/2}$) vs the current in µA of **2** (0.002 M) in THF using [^{n}Pr$_4$N][BAr$^F_4$] (0.1 M) as the electrolyte. Wave centered at −1.53 V (vs Fc/Fc$^+$).

5. Table S4. Summary of spectroscopy data for **1** and **2**

Spectra Data		**1**	**2**
	λ_{abs} /nm (ε M^{-1} cm^{-1})	472	477
	λ_{emi} /nm	495, 549	499, 551
Stokes shift (nm)		23	22
Φ		0.18	0.068
τ /ns		206	146
$k_r{}^a$/×10^6 s^{-1}		0.87	0.47
$k_{nr}{}^a$/×10^6 s^{-1}		3.90	6.38

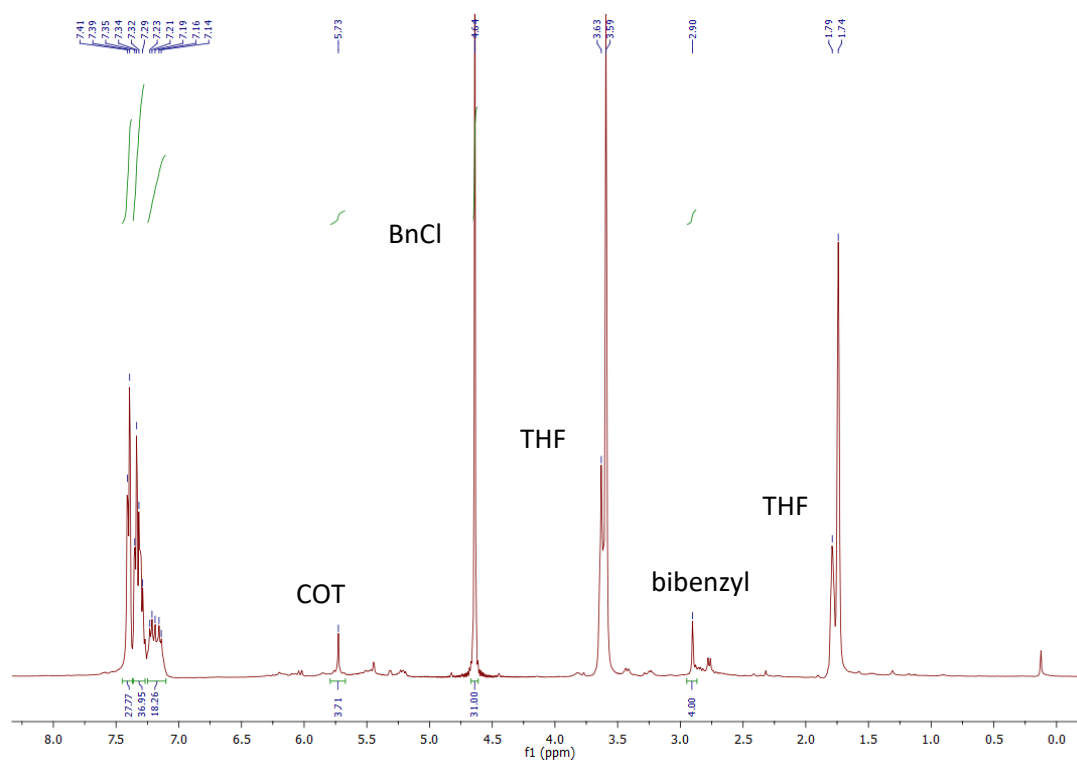a. $\Phi = k_r/(k_r + k_{nr})$, $\tau = 1/(k_r + k_{nr})$

6. Photoinduced dehalogenation reactions of benzyl chloride with 1 and 2

Figure S19: ^{1}H NMR (THF-d_8) spectrum of reaction mixture after reacting **1** with 10 equiv benzyl chloride under 467 nm irradiation for 24 h at RT.

Figure S20(a): ^{1}H NMR (THF-d_8) spectrum of reaction mixture after reacting **1** with 10 equiv benzyl chloride under dark condition for 24 h at RT.

Figure S20(b): ^{1}H NMR (THF-d_8) spectrum of XAT reaction of 10 equiv benzyl chloride irradiated with 467 nm light for 24 h at RT in absence of **1**.

Figure S21: ^{1}H NMR (THF-d_8) spectrum of reaction mixture after reacting **2** with 10 equiv benzyl chloride under 467 nm irradiation for 24 h at RT.
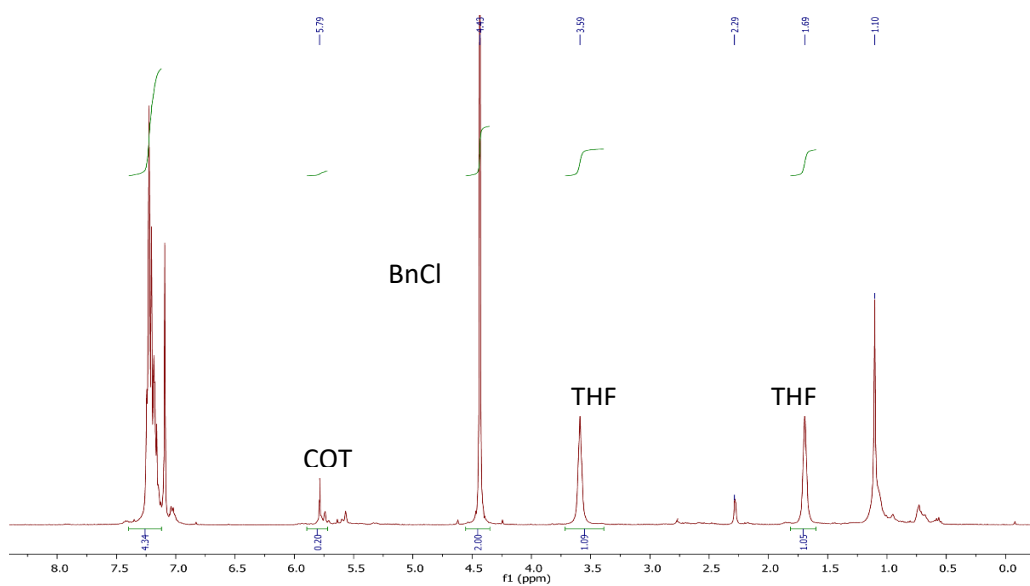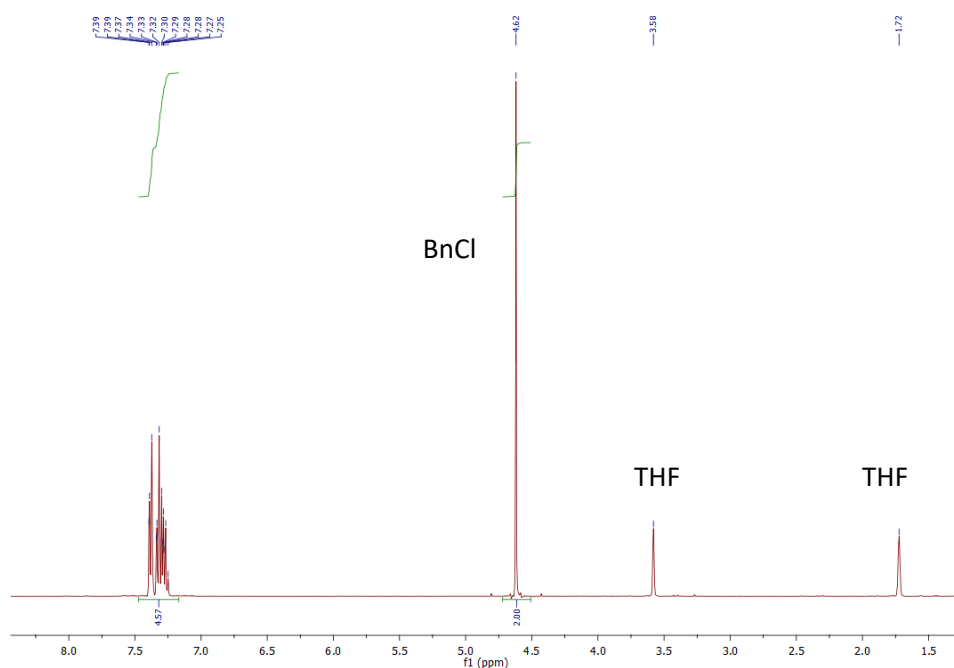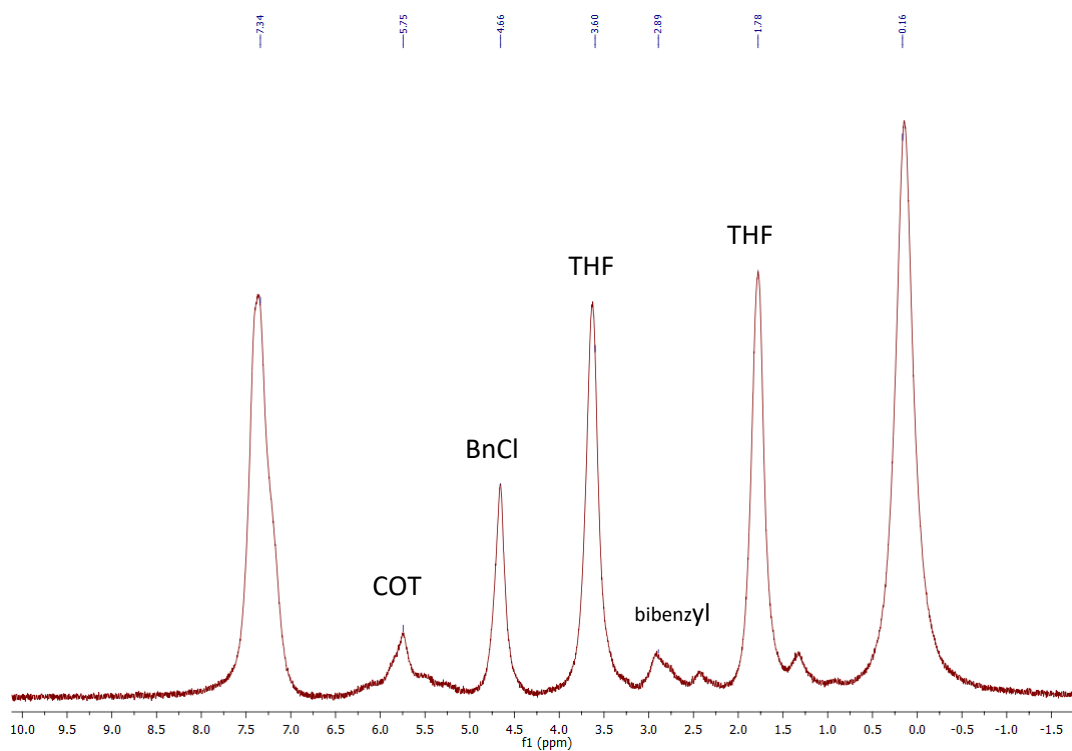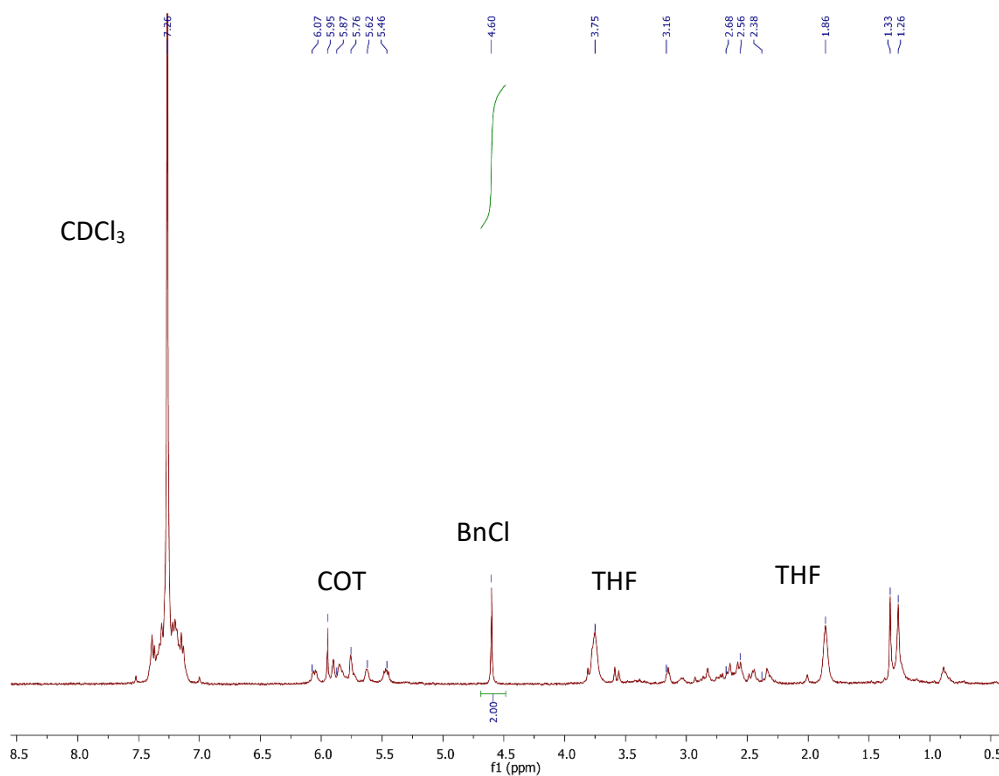
Figure S22: ^{1}H NMR (CDCl$_3$) spectrum of reaction mixture after reacting **2** with 10 equiv benzyl chloride under dark condition for 24 h at RT. (Reaction mixture was quenched with CH$_3$CN outside the box and NMR was taken in CDCl$_3$ due to poor solubility of complex **2**).

7. References

(1) U. Kilimann, M. Schäfer, R. Herbst-Irmer and F. T. Edelmann, *J. Organomet. Chem.*, 1994, **469**, C10-C14.

(2) K. Hodgson, F. Mares, D. Starks and A. Streitwieser, *J. Am Chem. Soc.* 1973, **95**, 8650-8658

(3) CrysAlisPro 1.171.41.107a: Rigaku Oxford Diffraction, Rigaku Corporation, Oxford, UK. (2020).

(4) CrysAlisPro 1.171.41.107a: Rigaku Oxford Diffraction, Rigaku Corporation, Oxford, UK. (2020).

(5) SCALE3 ABSPACK v1.0.7: an Oxford Diffraction program; Oxford Diffraction Ltd: Abingdon, UK, 2005.

(6) SHELXT v2018/2: Sheldrick, G.M., Acta Cryst., A, 71, 3-8 (2015).

(7) SHELXT v2018/2: Sheldrick, G.M., Acta Cryst., A, 71, 3-8 (2015).

(8) Hodgson, K. O.; Raymond, K. N. Dimeric .pi.-cyclooctatetraene dianion complex of cerium(III). Crystal and molecular structure of [Ce(C8H8)Cl.20C4H8]2. *Inorg. Chem.* 1972, **11** (1), 171-175.

(9) Yin, H.; Carroll, P. J.; Anna, J. M.; Schelter, E. J. Luminescent Ce(III) Complexes as Stoichiometric and Catalytic Photoreductants for Halogen Atom Abstraction Reactions. *J. Am. Chem. Soc.* 2015, **137** (29), 9234-9237.

(10) Lakowicz, J. R. Principles of Fluorescence Spectroscopy, 3rd Ed.; Springer: New York, 2006. 6.

(11) https://jascoinc.com/applications/quantum-yield-integrating-sphere/

(12) Suzuki, K.; Kobayashi, A.; Kaneko, S.; Takehira, K.; Yoshihara, T.; Ishida, H.; Shiina, Y.; Oishi, S.; Tobita, S. Reevaluation of absolute luminescence quantum yields of standard solutions using a spectrometer with an integrating sphere and a back-thinned CCD detector. *Physical Chemistry Chemical Physics* 2009, **11** (42), 9850-9860, 10.1039/B912178A. DOI: 10.1039/B912178A